

The Role of Reaction Engineering in Cancer Biology: Bio-Imaging Informatics Reveals Implications of the Plasma Membrane Heterogeneities

ABSTRACT

Recent developments in microscopy have led to revolutionary advances in our knowledge of the spatiotemporal dynamics of proteins in the plasma membrane of living cells and of heterogeneity of the plasma membrane. For example, spatial heterogeneities in the epidermal growth factor (EGF) receptor (EGFR) distribution in different domains of the plasma membrane are becoming increasingly evident. However, the influence of these heterogeneities on cellular signaling remains elusive despite uncontrolled receptor signaling being implicated in various forms of cancer. Herein, we suggest a reaction engineering, multiscale simulation framework, coined as model based bio-imaging informatics. This framework can fill in the scales' gap between various experimental methods and analyze the wealth of image informatics to unravel the influence of plasma membrane heterogeneities on the early events of the EGFR signaling, namely EGF binding and EGFR dimerization. An overarching conclusion arising from our work is that the plasma membrane heterogeneities can strongly modulate the amount as well the mechanism of ligand-receptor binding.

Keywords: multiscale modeling, kinetic monte carlo, receptors, diffusion, imaging, informatics, cancer

1. Introduction

The ErbB family of receptors triggers a rich network of signaling pathways and regulate cellular functions, such as proliferation, differentiation, and migration (Holbro and Hynes, 2004; Yarden and Sliwkowski, 2001). In higher vertebrates, the ErbB family of receptors consists of four members: epidermal growth factor (EGF) receptor (EGFR)/ErbB1/HER1, ErbB2/Neu/HER2, ErbB3/HER3, and ErbB4/HER4. A large number of studies have focused on the ErbB signaling network, not only because of their involvement in a variety of cellular processes, but also due to their role in a variety of human cancers (Yarden and Sliwkowski, 2001). Cancer appears as a tumor made up of a mass of cells as a result of uncontrolled signaling, in particular the signaling initiated by the ErbB family of receptors (Herbst, 2004; Holbro and Hynes, 2004; Normanno *et al.*, 2006; Yarden and Sliwkowski, 2001).

Since EGF binding represents the initial step for activating EGFR, considerable work has been devoted to elucidating the mechanisms of EGF binding and EGFR dimerization (Jorissen *et al.*, 2003; Klein *et al.*, 2004; Lemmon *et al.*, 1997; Sako *et al.*, 2000; Schlessinger,

1986;Wiley, 1988;Wiley *et al.*, 2003). A part from *in vitro* biochemical experiments to study the mechanisms of the EGFR activation (Jorissen *et al.*, 2003), recent developments in microscopy have made it possible to visualize protein dynamics in living cells (Weijer, 2003). These developments have led to revolutionary advances in our knowledge of the spatiotemporal dynamics of proteins in the plasma membrane (Kusumi *et al.*, 2005; Par-ton and Hancock, 2004).

Over 30 years ago, the two-dimensional continuum fluid mosaic model of the plasma membrane was proposed by Singer and Nicolson (1972). The model described the plasma membrane as a two-dimensional oriented solution of integral proteins in the viscous phospholipid bilayer. However, recent experimental data using fluorescence recovery after photobleaching (FRAP), single particle tracking, and optical laser trap methods suggest that the membrane proteins do not randomly diffuse in the plasma membrane (Jacobson *et al.*, 1995; Kusumi *et al.*, 2005) as thought previously. In contrast, a new model suggesting a compartmental picture of the plasma membrane is emerging. Several studies have indicated inhomogeneities in the plasma membrane and excellent reviews have been published on this topic including Ku-

* Corresponding author. Tel.: +1 302 831 2830; fax: +1 302 831 1048.

sumi *et al.* (2005), Kusumi and Sako (1996), Laude and Prior (2004), Parton and Hancock (2004), and Vereb *et al.* (2003). These studies have suggested localization of receptors within small regions, called microdomains, of the plasma membrane. In this picture, membrane proteins, such as EGFR, are confined in these microdomains and exhibit different spatial properties in terms of local EGFR density and local EGFR diffusivity (Murakoshi *et al.*, 2004; Murase *et al.*, 2004; Vereb *et al.*, 2003; Wilson *et al.*, 2004). Several studies have indicated that the lipid rafts and other cholesterol-rich regions of the plasma membrane can provide a localization platform to EGFR (Pike, 2003; Roy and Wrana, 2005).

While an increasing number of experimental studies are providing evidence of spatial heterogeneities of the plasma membrane itself and of the EGFR distribution (Kusumi *et al.*, 2005; Laude and Prior, 2004; Lommerse *et al.*, 2004; Maxfield, 2002; Pike, 2003; Wilson *et al.*, 2004), the influence of these heterogeneities on cellular signaling remains elusive. Despite computational efforts to model ligand dynamics, receptor dynamics, and receptor trafficking (see Goldstein *et al.*, 2004; Haugh, 2002; Kholodenko, 2006; Lauffenburger and Linderman, 1993; Mayawala *et al.*, 2006; Monine *et al.*, 2005; Monine and Haugh, 2005; Pribyl *et al.*, 2003; Shvartsman *et al.*, 2004; Woolf and Linderman, 2003 and references therein), only a few efforts, to the best of our knowledge, have considered the influence of plasma membrane heterogeneities on EGFR signaling; see Mayawala *et al.* (2005a,b) and Mayawala *et al.* (2006) and references therein. More importantly, the wealth of information provided from modern imaging techniques has not yet been analyzed in a quantitative manner.

In this paper, we propose a reaction engineering based computational framework for the integration of biochemical and imaging experimental data. Our focus is to analyze the influence of plasma membrane heterogeneities on the early events of the EGFR signaling, namely

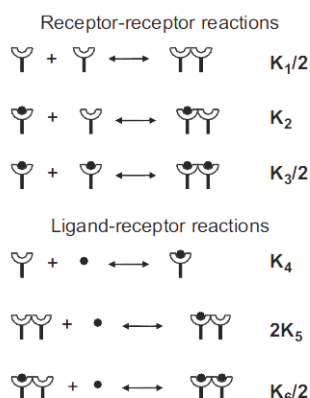


Figure 1. Reactions of EGF binding and EGFR dimerization. Reprinted by permission of Federation of the European Biochemical Societies from Mayawala *et al.* (2005a), copyright 2005.

EGF binding and EGFR dimerization, by providing an overview of our recent work. The organization of this paper is as follows. First, an equilibrium model is employed to examine the effect of plasma membrane heterogeneity on the uptake data of the ligand on the receptor. Next, dynamic models are discussed. A simple criterion is proposed to delineate whether one should use well-mixed vs. distributed models and continuum vs. discrete models. The first comparison to single particle experimental data is presented. Finally, conclusions are drawn.

2. Model Based Bio-Imaging Informatics: A Framework for Integrating and Analyzing Experimental Data

The EGF–EGFR reaction network is shown in Figure 1. The network entails (i) binding (adsorption) to and detachment (desorption) of ligand (L) on free or unbound receptors (R), and their dimers (RR and RRL), (ii) dimerization reactions between receptors and their reverse, and (iii) diffusion of receptors and their dimers within the plasma membrane. Note that part of the receptor is in the extracellular medium, part in the intracellular medium, and the rest within the membrane. These reaction–diffusion processes are typical of catalytic reactions and more generally of reaction engineering, and application of such models to biological systems can be invaluable.

The reaction network involves processes occurring on a wide range of time and length scales, as shown in Figure 2. The disparity in time scales is due to a wide range of reaction rate constants and diffusion. For the latter, there is a characteristic microscopic time scale for diffusion from one site to the next (as the receptors exchange positions with the lipids of the membrane, Eisinger *et al.*, 1986). This exchange process results in diffusivity values, which are much lower than those encountered in solution and are more reminiscent of the values of activated surface diffusion on catalysts. Furthermore, there is a macroscopic time scale determined from the distance between receptors and the microscopic diffusion time scale. This macroscopic time scale can be much larger than the microscopic one due to the very low density of receptors on the plasma membrane. This point is further elaborated below. The length scale disparity arises from the difference in the size of a receptor ($\sim 1\text{--}10$ nm in diameter) and the size of the cell ($\sim 10\text{--}50$ μm in diameter). Such disparity in length and time scales seriously plagues both experimental and first-principles modeling efforts.

More traditional imaging methods, such as electron microscopy (EM) experiments using immunogold labeling (Miller *et al.*, 1986; Vanbelzen *et al.*, 1988) and covalent linking to chemical conjugates like ferritin (Haigler *et al.*, 1979), have a high spatial resolution but

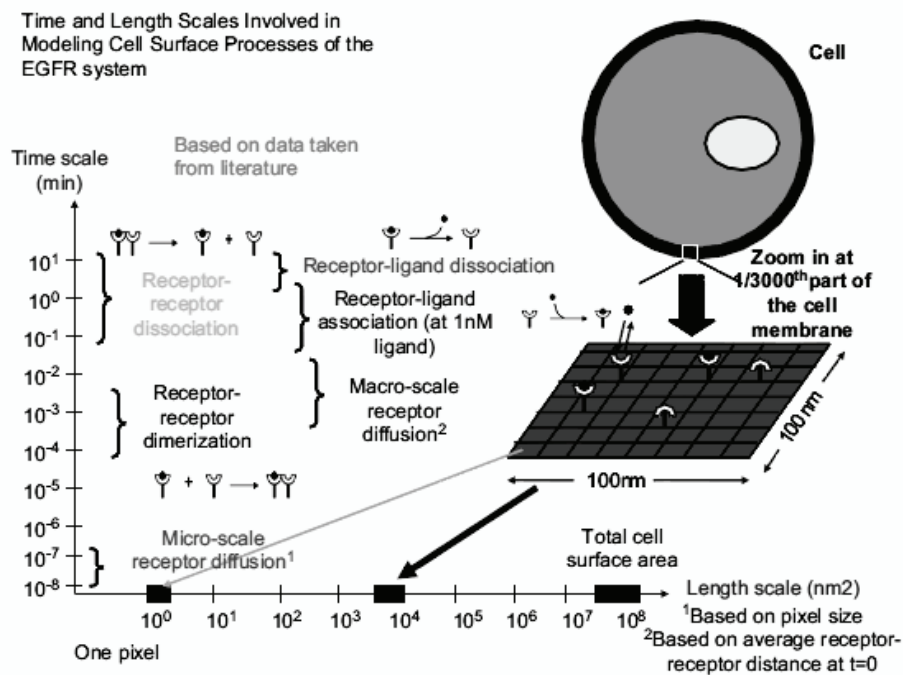


Figure 2. Length and time scales involved in the cell surface events of the EGFR signaling. Multiple length and time scales of the system make conventional Monte Carlo algorithms for spatiotemporal modeling highly inefficient.

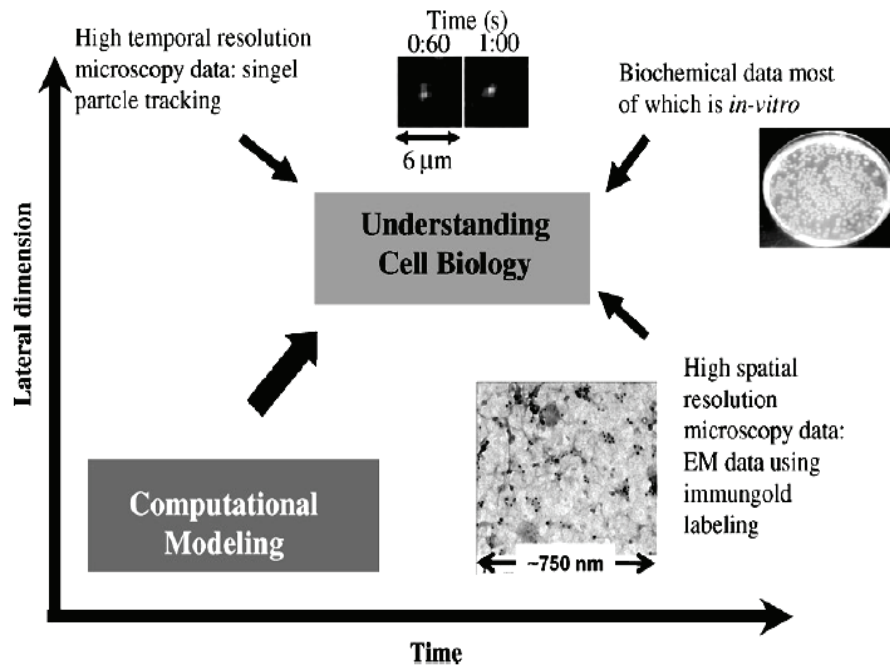


Figure 3. A time-length scale graph of the proposed approach of bio-imaging informatics. Computational integration of low spatial and temporal resolution biochemical data with high temporal resolution (single particle tracking e.g., Sako *et al.*, 2000) and high spatial resolution (electron microscopy, e.g., Vanbelzen *et al.*, 1988) imaging data. The images of the single particle tracking and electron microscopy have been reprinted by permission from the Macmillan Publishers Ltd: Nature Cell Biology (Sako *et al.*, 2000), copyright 2000, and the Rockefeller University Press: Journal of Cell Biology (Miller *et al.*, 1986), copyright 1986.

no dynamics information (see Figure 3). Recently introduced imaging methods, such as fluorescence confocal

microscopy (Verveer *et al.*, 2000), single particle tracking. (Sako *et al.*, 2000), and quantum dot based ligands

(Lidke *et al.*, 2004), have high temporal resolution but a relatively low spatial resolution (of the order of ~ 0.2 – $0.5\mu\text{m}$), as shown in Figure 3, due to their optical nature.

These methods exhibit high sensitivity, i.e., one can visualize individual proteins in a spot, but it is not unambiguously clear when many proteins are nearby. As a result, available imaging technologies do not allow simultaneous high temporal and spatial resolution of multiple receptors. Traditional *in vitro* experimental techniques (see Figure 3) provide no spatial information (they typically give spatial average and often population average, i.e., over multiple cells, coarse-grained data). At the same time, such experiments are relatively easy to conduct, and have been and will continue to be the backbone of biochemical experimentation.

The above comments underscore the fact that currently there is not a single experimental technique that simultaneously spans all length and time scales. Yet, imaging provides a wealth of spatial and/or temporal informatics at intermediate or mesoscopic length and time scales. Unfortunately, all this information is difficult to interpret using Qualitative models. The application of chemical engineering principles can be invaluable in extracting quantitative information to better elucidate the mechanisms by which plasma membranes behave.

While further advances in experimentation should be expected in the future, the aforementioned experimental limitation creates a true opportunity for the emerging field of multiscale modeling that links models at various scales (Vlachos, 2005). To integrate these imaging data along with biochemical data, we propose an approach, coined as *model based bio-imaging informatics*, which is depicted in Figure 3. We propose that multiscale models could be used to fill in the scales' gap between the various experimental methods and integrate multiple experimental data with the objective of understanding signaling, reconciling various experimental data, and eventually proposing experiments and increasing our understanding of cancer. Some of these efforts of our group are reviewed below.

A natural question raised is which are the suitable scales and corresponding models of the multiscale ladder for studying plasma membrane phenomena. *In vivo* microscopy emphasizes the need for computational tools that at least consider spatial heterogeneity. A patch model (reminiscent of adsorption in heterogeneous adsorbates and catalysts) is the simplest approach that can account for spatial heterogeneity and is discussed in the next section. Single molecule imaging points to the need for discrete rather than the traditional continuum and often well-mixed representation. Furthermore, the spatial heterogeneity of the plasma membrane and of the proteins (e.g., cluster formation at longer times, uphill diffusion, etc., which are not further discussed here) underscores the possible inability of continuum spatial models, such as reaction–diffusion models, for quantitative modeling of these phenomena. Therefore, the most suitable ap-

proach for modeling mesoscopic scale phenomena in the plasma membrane is a kinetic Monte Carlo (KMC) tool (Chatterjee *et al.*, 2004). This method has successfully been used in catalysis since the 1980s (Ziff *et al.*, 1986) and provided insights into spatial correlations, fluctuations, and phase transitions. However, direct application of KMC simulation to biological systems is impractical. We elaborate on this important issue next. We return to the suitability of various kinetics-transport models later. Extension of mesoscale models to smaller and larger scales is obviously very important and should be considered in future work.

2.1. Spatial KMC Mesoscopic Simulation

Stochastic simulation of reaction–diffusion systems is one of the most detailed but also most expensive mesoscopic tools for studying surface phenomena (Chatterjee *et al.*, 2004). It can be computationally prohibitive with biologically relevant parameters, as indicated in Figure 2, due to the large disparity in length and time scales. As a result, most biological simulations have employed only a very small number of reactions (this is in contrast to the combinatorial explosion of actual problems) and parameters of comparable magnitude only. One of the major factors contributing to the high computational cost arises from the low density of receptors making the macroscopic time scale for diffusion long (this is a relatively unique feature of biological systems). Furthermore, the separation of reaction time scales, a phenomenon known as stiffness, plagues traditional KMC simulation. The execution of one event at a time (instead of simultaneously advancing all species) is another obstacle of KMC. Finally, efficient implementation (search and update) strategies can substantially affect computational speed and programming ease. Recent approaches on accelerated KMC methods hold promise for overcoming these challenges. These efforts, by our group and others, are reviewed in Chatterjee and Vlachos (2007) and Vlachos (2005) and will not be repeated here.

Some comments regarding algorithmic implementation are worth discussing briefly. Two main approaches for spatial KMC implementation are the null-event and the rejection-free algorithms (Chatterjee and Vlachos, 2007; Reese *et al.*, 2001). In this work, we selected the null-event KMC algorithm mainly due to its implementation ease, and devised an improvement to handle the low density of receptors (a hybrid null-event algorithm). In the traditional null-event algorithm (e.g., Reese *et al.*, 2001; Ziff *et al.*, 1986), a site is randomly picked. If the selected site is occupied, then the transition rates of all the microprocesses that can occur on the selected site are computed. The transition rates are normalized with a predefined maximum transition rate to calculate probabilities. Based on these probabilities, a microprocess may or may not (null-event) be selected to occur. At low receptor densities, the null-event algorithm is computationally intensive because low density implies a large

probability of null events by mostly picking empty sites of the lattice.

In our hybrid null-event algorithm, instead of randomly picking lattice sites, we randomly pick only among the occupied sites by simply tracking the occupied sites. This is then a hybrid approach that combines the ease of implementation of a null-event algorithm with the success rate of a rejection-free algorithm. Corresponding to typical densities encountered for receptors in the plasma membrane, Figure 4 shows that this modification can lead to over *four* orders of magnitude speed up, depending on receptor density, over the conventional null-event KMC method. This point illustrates that even small algorithmic improvements can have a tremendous impact on our ability to model biological systems.

3. An Equilibrium Model to Integrate Biochemical and Electron Microscopy Data

Recently, we analyzed the influence of the plasma membrane heterogeneities on the EGF binding to EGFR by a loose integration of electron microscopy data and biochemical data using a very simple equilibrium model (Mayawala *et al.*, 2005a). The Scatchard method (briefly mentioned in Appendix A) has extensively been used to analyze the experimental data of equilibrium EGF binding to EGFR (Klein *et al.*, 2004; Wofsy and Goldstein, 1992; Wofsy *et al.*, 1992; Zidovetzki *et al.*, 1991). In a simplistic way, the Scatchard equation, similar to the well-known Langmuir isotherm for adsorption of species on solid catalysts, describes the isotherm of ligand binding to receptors by appropriately linearizing the equation. The data show a concave-up shape, as shown in Figure 5, in contrast to the concave-down shape predicted using typical equilibrium constants (Wofsy *et al.*, 1992). While several studies have provided arguments to explain the concave-up shape, the mechanism responsible for the concave-up nature has been a controversial issue for over a decade (Chamberlin and Davies, 1998; Holbrook *et al.*, 2000; Klein *et al.*, 2004; Wofsy and Goldstein, 1992).

Motivated by electron microscopy and biochemical data, we hypothesized that heterogeneity in the local density of the EGFR, due to localization in certain regions of the plasma membrane, can lead to a concave-up Scatchard plot of the EGF/EGFR system. In general, there can be multiple domains with multiple receptor densities. Our model assumed a simplified representation of the receptor density heterogeneity by dividing the plasma membrane into two domains of different receptor densities (a simple two patch model). The total binding was calculated as the binding in low- and high-density regions.

We compared the heterogeneous receptor density model with the experimental data of EGF binding to EGFR in A-431 cells. Figure 5 compares the fitted heterogeneous receptor density model with the experimental data of Zidovetzki *et al.* (1991). Fairly good agreement is seen. At low EGF concentrations, binding takes place predominantly in the high EGFR density regions because

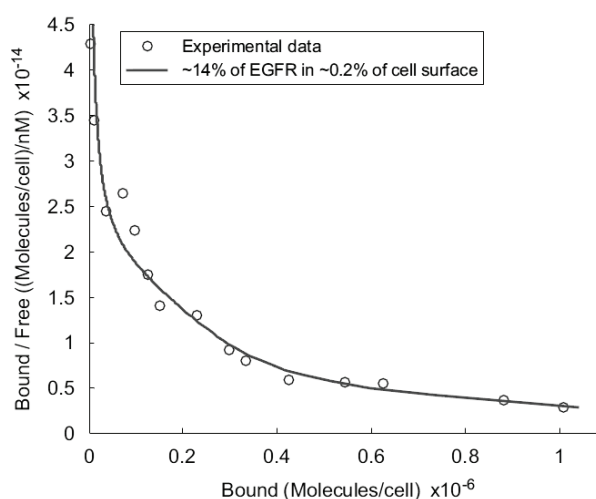


Figure 4. The Scatchard plot: comparison of the heterogeneous receptor density model against experimental data (Zidovetzki *et al.*, 1991). The equilibrium parameters are: $K1 = 2.19M^{-1}$, $K2 = 1.02 \times 10^3 M^{-1}$, $K3 = 4.77 \times 10^5 M^{-1}$, $K4 = 6 \times 10^6 M^{-1}$, $K5 = K6 = 2.8 \times 10^9 M^{-1}$. Reprinted by permission of Federation of the European Biochemical Societies from Mayawala *et al.* (2005a), copyright 2005.

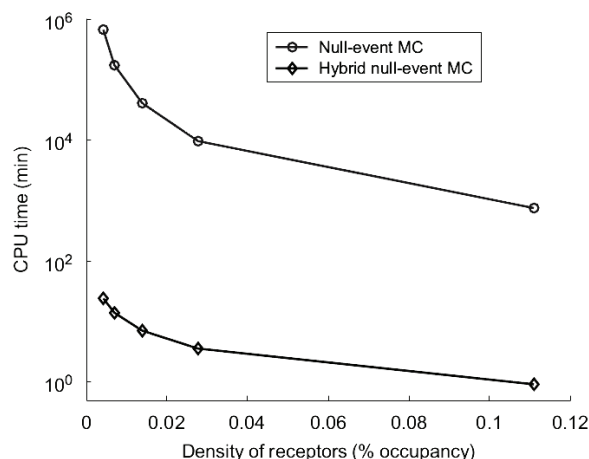


Figure 5. Comparison of CPU (min) of null-event KMC and hybrid null-event KMC algorithms on a 600×600 lattice at five different low densities for executing 4×10^5 collisions. Density indicates the surface coverage. The values for null-event KMC were calculated for 400 collisions and then scaled for 4×10^5 collisions. The top curve shows that simulation of low receptor density systems is impractical using the conventional null-event KMC algorithm. The curves show CPU savings of $\sim 30,000$ (at the lowest density of 0.004%) to 800 (at the highest density shown of 0.11%). For each data point, 10 simulations with different seeds of the random number generator were used to collect statistics. Simulations were performed on an AMD_2000+ MP processor.

of the presence of more predimerized EGFR. As the concentration of the EGF increases, the high-density re-

gions get saturated and binding takes place in low-density regions, containing mainly EGFR monomers.

The data were fitted assuming a localization of $\sim 14\%$ of the EGFR in 0.17% of the plasma membrane. These numbers are not unique and depend on the equilibrium constants (which have not been determined based on a heterogeneous model). The suggested extent of localization lies, at least qualitatively, in the range suggested by biochemical and electron microscopy studies. More important than the specific numbers is that it was found that the concave-up shape is preserved over a wide range of localization as well as equilibrium parameters (Mayawala *et al.*, 2005a). In future work, we propose obtaining microscopy data to characterize the effect of heterogeneity of the plasma membrane and receptor density in microdomains and extract equilibrium constants from the Scatchard plot, i.e., to carry out the analysis in the reverse way from what we have done so far to obtain intrinsic equilibrium constants.

This first computational analysis highlights the influence of the plasma membrane heterogeneity on EGFR signaling, and serves as a motivation for further kinetics-transport analysis discussed next.

4. Dynamic Modeling

4.1. Choosing a Suitable Mesoscopic Model

As alluded to above and further discussed in Chatterjee *et al.* (2004) and Vlachos (2007), at each scale there is a hierarchy of models, which vary in complexity, computational cost, and accuracy. It is therefore important to develop simple criteria that can guide model selection within a scale to strike a balance between accuracy and computational cost. With this as a motivation, in this section first we assess the importance of spatial phenomena and then we evaluate the accuracy of partial differential equations (PDEs) in transient situations (e.g., upon an extracellular stimulation via exposure of cells to ligand) when spatial effects are important.

In order to evaluate the importance of spatial effects on overall kinetics in two-dimensional bimolecular reactions *a priori* (i.e., without performing spatial simulations), we have assessed the applicability of the second Damkohler number (Da), defined here as the ratio of time scales of collision between receptors and reaction. For a bimolecular (dimerization) reaction $A + B \rightarrow AB$, using the mean-field approximation, the Da number can be defined as (Mayawala *et al.*, 2006)

$$Da = \frac{\text{time scale of collision event}}{\text{time scale of reaction event}} = \frac{1/4D_{AB}/s^2}{1/k_f} = \frac{k_{f,Areal}}{4D_{AB}} \quad (1)$$

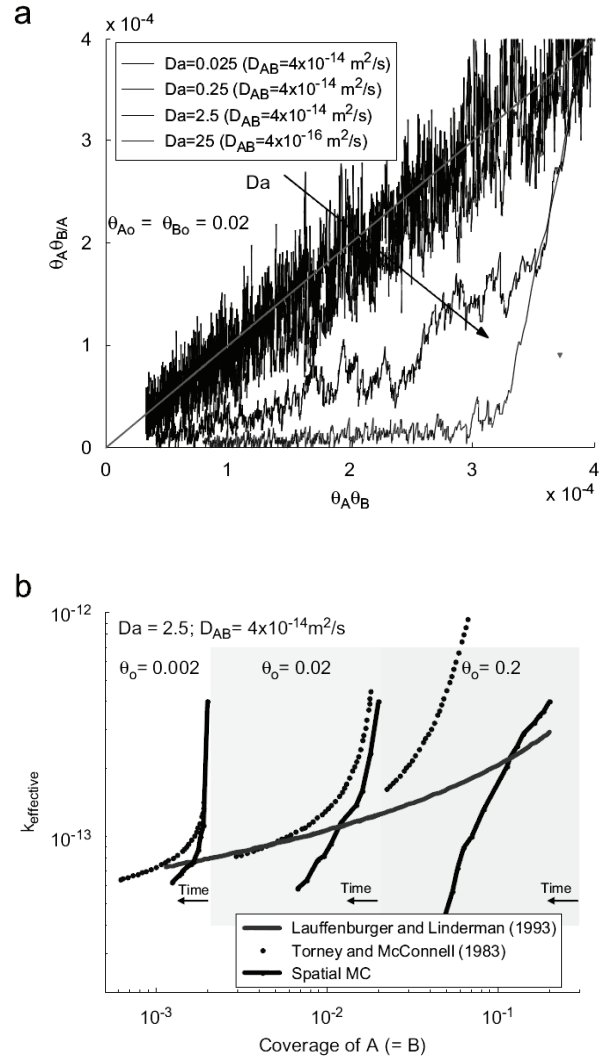


Figure 6. (a) $\theta_A \theta_{B/A}$ VS. $\theta_A \theta_B$ for Da numbers in the range of 0.025–25 and an initial receptor coverage of $\theta_{A0} = \theta_{B0} = 0.02$ (subscript 0 denotes initial conditions). $\theta_A \theta_{B/A} = \theta_A \theta_B$ follows the diagonal. (b) Comparison of effective rate constant vs. time, obtained using the spatial KMC and two simple PDE models, for three different initial coverages and $Da = 2.5$. Curves represent the mean of 30 concentration profiles obtained using different random number seeds. Reprinted with permission from Elsevier from Biophysical Chemistry (Mayawala *et al.*, 2006).

where $D_{AB} = D_A + D_B$, D_A and D_B are the diffusivities of A and B , respectively, k_f and $k_{f,Areal}$ are the intrinsic reaction rate constants for a bimolecular reaction between A and B in units of (receptors/site) $^{-1}$ s $^{-1}$ and (receptors/area) $^{-1}$ s $^{-1}$, and s is the encounter radius. k_f and $k_{f,Areal}$ are related using the encounter radius, as follows:

$$k_{Areal} = ks^2 \quad (2)$$

To test the Da number criterion and ensure the lack of

finite size effects, spatial KMC simulations were performed, described in Mayawala *et al.* (2005b, 2006).

Let θ_i be the coverage of species i and $\theta_{B/A}$ be the conditional probability of picking B given that the first chosen site is occupied by A . When spatial correlations are unimportant, then $\theta_A\theta_{B/A} = \theta_A\theta_B$, and the dynamics can be described using a well-mixed model. Deviations from $\theta_A\theta_{B/A} = \theta_A\theta_B$ provide a measure of the importance of spatial correlation effects.

Figure 6(a) compares $\theta_A\theta_{B/A}$ VS. $\theta_A\theta_B$ for an initial density of 0.02 for both A and B , and Da numbers in the range of 0.025–25. For a low value of $Da=0.025$, $\theta_A\theta_{B/A} = \theta_A\theta_B$ is indicative of a well-mixed situation. An increase in the Da number leads to inability of diffusion to homogenize spatial correlations (Vlachos, 2005). In the receptor density range of interest (10^2 - 10^5 receptors per μm^2), we have found that dimerization reactions in the plasma membrane with $Da > \sim 0.1$ require spatial modeling (Mayawala *et al.*, 2006). This criterion, based on a standard dimensionless group, indicates that the separation of time scales between diffusion and reaction can be an efficient means of deciding whether a well-mixed or a spatially distributed model should be chosen.

Since PDE models could be used for spatial modeling, next we have investigated differences between PDE and KMC predictions. Two simple analytical PDE models were used. First a quasi-steady state model by Lauffenburger and Linderman (1993) and second a transient model by Torney and McConnell (1983) (for details see Mayawala *et al.*, 2006). Fig. 6(b) shows up to two orders of magnitude difference in the transient effective reaction rate constant of a bimolecular activation between simple PDEs and spatial KMC. Furthermore, this simulation indicates that the effective reaction rate constant depends on initial conditions (e.g., cluster density) and plasma membrane heterogeneity (e.g., different density of receptors in various microdomains). Thus, estimation of intrinsic parameters from experimental data should pay particular attention to these issues.

This comparison shows that a spatial KMC model is needed to capture the creation of a spatially non-random distribution of proteins due to bimolecular reactions. Furthermore, a spatial KMC model can also easily consider the spatial heterogeneity of the plasma membrane due to microdomains, and the noise resulting from a small number of copies of activated receptors. Thus, the KMC method is a natural framework for mesoscopic modeling of biological phenomena on the plasma membrane when spatial effects are deduced to be important.

4.2. Kinetic Modeling of the EGFR Dimerization and the EGF Binding

The EGF binding can take place with three different reaction paths. Path 1 (reactions 1, 5, and 6; see Figure 1)

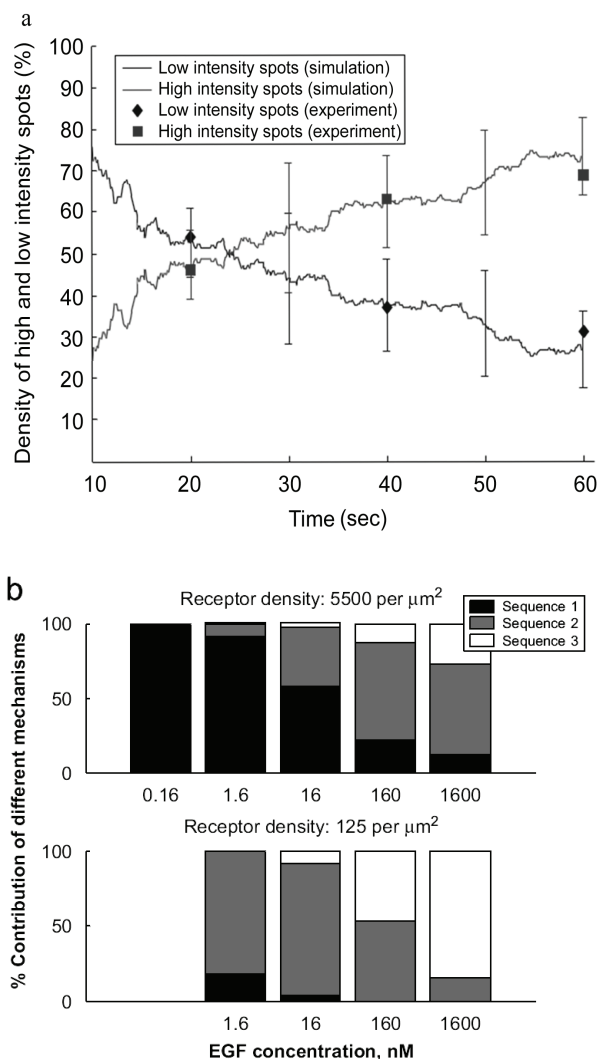


Figure 7. (a) Evolution of high intensity spots representing $(\text{EGF}\cdot\text{EGFR})_2$ and low intensity spots representing $\text{EGF}\cdot\text{EGFR}+\text{EGF}\cdot(\text{EGFR})_2$ obtained using our simulations along with the data of single particle tracking experiments by Sako *et al.* The simulations were performed for a receptor number density of 5500 per μm^2 and 18% dimers initially. The simulation intensity has been normalized with the experimental data. © 2005 from Mayawala *et al.*; licensee BioMed Central Ltd. (b) Contributions of the different reaction mechanisms at 60 s as a function of EGF concentration with a receptor number density of 5500 and 125 receptors per μm^2 . The bars indicate the mean obtained from 10 independent KMC simulations.

entails dimerization of unbound receptors followed by ligand binding. Path 2 (reactions 4, 2, and 6; see Figure 1) entails dimerization of an unbound and a bound receptor followed by ligand binding. Sequence 3 (reactions 4 and 3; see Figure 1) entails dimerization of bound receptors. Recently, we analyzed the relative contribution of these paths in EGFR dimerization (Mayawala *et al.*, 2005b). Details on simulation size and model parameters are given in Appendix B. Corresponding to the EGFR dimerization events, the Da number ranges between 10^{-4} and 1.

The dynamics of the ligand binding events were compared with the single particle tracking experiment of Sako *et al.* (2000) at a low EGF concentration of 0.16nM in the 0.60 s time interval as shown in Figure 7(a). The predicted increase of low intensity spots, representing monomers plus dimers having one EGF bound, and high intensity spots, representing EGFR dimer with two EGF molecules, is qualitatively consistent with the experimental data. In agreement with the experiments of Sako *et al.* (2000), path 1 was found to be dominant, contributing 95–100% in the formation of the bound–unbound receptor (EGF.EGFR)₂. This comparison serves as a model validation step.

Single particle tracking experiments are typically limited to low ligand concentrations (Sako *et al.*, 2000). High concentration of ligand would lead to fluorescence of a large number of EGFRs making it impossible to visualize individual particles. However, simulations can be used to overcome the limitation. Our simulations indicate that the relative contributions of paths 1–3 at 60 s change with ligand concentration (see Figure 7(b)). At low ligand concentration, path 1 dominates, whereas at higher ligand concentration, a significant fraction of dimers form via path 2 as well as path 3. At low ligand concentration, most of the ligand binds to predimerized receptors with higher affinity; however, the extent to which free EGFR dimerization can occur is limited due to the low affinity of free EGFR dimerization. At higher ligand concentration, at least one of the dimerization partners is ligand bound.

The receptor density can also significantly influence the mechanism of EGF binding as shown in Figure 7(b). For a low receptor density of 125 receptors per μm^2 , at lower EGF concentration path 2 is dominant, whereas at higher EGF concentration, path 3 is dominant. Path 1 is not important at low receptor density because of the low or negligible amount of predimerized EGFR.

Next, we analyzed the influence of spatial inhomogeneities on the dynamics of receptor dimerization as described in Mayawala *et al.* (2006) using a reversible dimerization reaction $A + B \rightarrow AB$. This reaction can represent EGFR dimerization between bound and unbound receptors or heterodimerization between two members of the ErBb family. We considered changes in EGFR density, due to different cell lines as well as due to localization, and in EGFR diffusivity. The variations in Da number in Figure 8 capture different reaction rate constants of different dimerization reactions shown in Figure 1, and different diffusivities, e.g., the highest Da number corresponds to fast dimerization of ligand bound monomer EGFR in the plasma membrane microdomains with reduced mobility.

Figure 8 shows that the diffusion limitation can significantly lower the dimerization rate in cell lines with a normal density as well as higher density (e.g., human A-431 epidermoid carcinoma cells) of EGFR. For normal cells, even a 100-fold higher density results in only \sim

2.3-fold increase in the diffusion limited dimerization rates (compare bottom and middle curves in Figure 8). This indicates that localization is unlikely to cause a significant increase in diffusion limited EGFR dimerization rates in normal cells. However, comparison of the middle and top curves in Figure 8 shows that in A-431 cells, only a 10-fold higher density leads to 1–2 orders of magnitude increase in the dimerization rate, suggesting that the dimerization rate is greatly enhanced due to localization. Obviously, this is a simple reaction network but illustrates the potential effect of spatial heterogeneity on signaling; more work is needed to exploit these effects in the full reaction–diffusion network of EGF–EGFR and other receptors. Future study is also needed to explicitly link these observations to their effect on intracellular signaling events.

5. Conclusions

This work proposes that multiscale modeling can be indispensable in filling the gap between various imaging and biochemical methods. Multiscale modeling can capitalize on the imaging informatics and provide unprecedented quantitative understanding of biological phenomena. Our initial work, reviewed in this paper, has already underscored the importance of plasma membrane heterogeneities on the EGF binding and the EGFR dimerization. Our work serves as a proof of concept of the feasibility of such simulations despite the disparity in scales and to reconcile apparent discrepancies between *in vitro* and *in vivo* experiments (e.g., on the cooperativity of the ligand binding). Obviously, the success of our model does not prove its correctness. Rather, the conclusions of this paper serve as hypotheses for future experiments. Such iterative approaches have been discussed in Aldridge *et al.* (2006) and Ma'ayan *et al.* (2005). For example, based on our equilibrium calculations, a future experiment could entail change of the cholesterol levels in the plasma membrane to observe its effect on the Scatchard plot. Experimental protocols for changing cholesterol levels have previously been developed (Pike, 2003). If the plasma membrane heterogeneities influence the EGF binding, then changing the cholesterol levels should change the distribution of the EGFR, leading to a possible shape change of the Scatchard plot. It is typically from a disagreement between model predictions and experimental data where one learns the most. Work along these lines is in progress.

6. Acknowledgments

This work was supported by grants from the US Department of Energy (DE-FG02-05ER25702) and the National Science Foundation (CTS-0343757). We are thankful to Bridget S. Wilson (Department of Pathology, University of New Mexico, Albuquerque, NM, USA) for providing us the unpublished electron microscopy image.

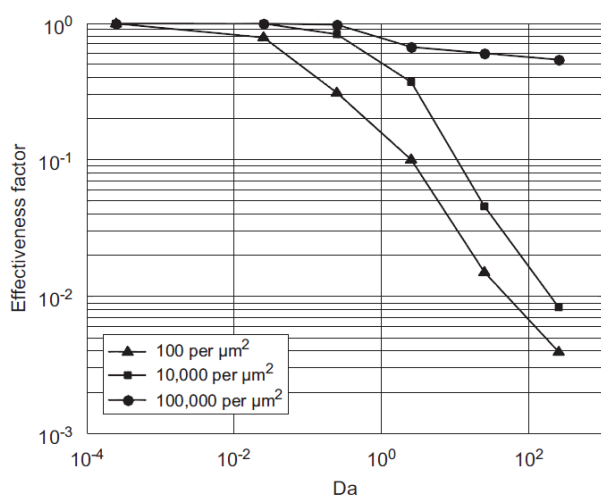


Figure 8. Effectiveness factor as a function of Da number calculated at 33% of the equilibrium concentration of the dimer produced from the reversible dimerization reaction between EGFR. Different dimerization events shown in Figure 1(a) are described by different Da number. Different diffusivities in different microdomains on the plasma membrane also contribute to Da number variation. The densities reported on the plot are the initial densities. The bottom curve is representative of an average EGF receptor density in typical normal cells, the middle curve of localization in normal cells and of an average EGF receptor density in cancer cells, and the top curve of localization in cancer cells. The points represent the mean of 30 concentration profiles obtained using different random number seeds and the lines just connect the points. Reprinted with permission from Elsevier from *Biophysical Chemistry* (Mayawala *et al.*, 2006).

7. Appendix A. The Scatchard Method

The Scatchard method involves a transformation of ligand–receptor binding data (an isotherm) such that the ratio of bound receptor (B) to free ligand (L) concentration when plotted as a function of bound ligand concentration gives a linear relation with a slope of $.Ka$ (association constant) and an intercept as the total density of sites RT (in the same units as B) (Scatchard, 1949),

$$\frac{B}{L} = -K_a B + K_a R_T \quad (\text{A.1})$$

8. Appendix B. Simulation Size and Model Parameters for KMC Simulations

The cell surface was represented using a two-d imensional square lattice with each pixel of $2 \text{ nm} \times 2 \text{ nm}$ in size. The number density of receptors ranges from $\sim 10^2$ receptors per μm^2 on normal cells (Benveniste *et al.*, 1988) to $\sim 10^3$ receptors per μm^2 on A-431 cells which overexpress EGFR (Wiley, 1988). However, the local density of receptors can be much higher *in vivo* because of the localization of receptors in certain regions of the plasma

membrane, such as in lipid rafts (Laude and Prior, 2004; Pike, 2003; Simons and Toomre, 2000). To represent normal cells with 125 receptors per μm^2 , we simulated a low density of 31 receptors on a $500 \text{ nm} \times 500 \text{ nm}$ mesh, and to represent A-431 cells with 5500 receptors per μm^2 , 55 receptors were randomly placed on a $100 \text{ nm} \times 100 \text{ nm}$ mesh. The diffusivity of monomer EGFR has been reported to be around $2 \times 10^{-14} \text{ m}^2 \text{ s}^{-1}$ (Kusumi *et al.*, 1993; Rees *et al.*, 1984). The model parameters are summarized in Mayawala *et al.* (2005b). We assumed two types of EGF binding on the cell surface: low affinity binding on monomer EGFR and high affinity binding on dimerized EGFR.

Based on experimental studies (Gadella and Jovin, 1995; Martin-Fernandez *et al.*, 2002; Moriki *et al.*, 2001; Vanbelzen *et al.*, 1988; Yu *et al.*, 2002), a fraction ($\sim 18\%$) of receptors was initially placed at random locations as dimers on simulated A-431 cells. Corresponding to the dimerization equilibrium constant for these data, there is a negligible number of dimers in the absence of ligand at a density of 125 receptors per μm^2 . The receptor dimerization constants vary with ligand occupancy. Several experimental studies have shown that dimerization occurs with higher affinity if at least one of the receptors is ligand bound. Finally, the highest affinity has been suggested for dimerization between two ligand bounded receptors (Lemmon *et al.*, 1997; Sherrill and Kyte, 1996).

REFERENCES

- [1] Aldridge, B.B., Burke, J.M., Lauffenburger, D.A., Sorger, P.K., 2006. Physicochemical modelling of cell signalling pathways. *Nature Cell Biology* 8, 1195–1203.
- [2] Benveniste, M., Livneh, E., Schlessinger, J., Kam, Z., 1988. Overexpression of epidermal growth factor receptor in NIH-3T3-transfected cells slows its lateral diffusion and rate of endocytosis. *Journal of Cell Biology* 106 (6), 1903–1909.
- [3] Chamberlin, S.G., Davies, D.E., 1998. A unified model of c-erbB receptor homo- and heterodimerisation. *Biochimica et Biophysica Acta (BBA)—Protein Structure and molecular Enzymology* 1384 (2), 223–232.
- [4] Chatterjee, A., Vlachos, D.G. 2007. A review of spatial microscopic and accelerated kinetic Monte Carlo methods for materials' simulation. *Journal of Computer-Aided Materials Design*, invited, in press.
- [5] Chatterjee, A., Snyder, M.A., Vlachos, D.G., 2004. Mesoscopic modeling of chemical reactivity (invited). *Chemical Engineering Science* 59, 5559–5567.
- [6] Eisinger, J., Flores, J., Petersen, W., 1986. A milling crowd model for local and long-range obstructed lateral diffusion. Mobility of excimeric probes in the membrane of intact erythrocytes. *Biophysical Journal* 49 (5), 987–1001.
- [7] Gadella Jr., T., Jovin, T., 1995. Oligomerization of epidermal growth factor receptors on A431 cells studied by time-resolved fluorescence imaging microscopy. A stereochemical model for tyrosine kinase receptor activation. *Journal of Cell Biology* 129 (6), 1543–1558.
- [8] Goldstein, B., Faeder, J.R., Hlavacek, W.S., 2004.

- Mathematical and computational models of immune-receptor signalling. *Nature Reviews Immunology* 4 (6), 445–456.
- [9] Haigler, H., McKanna, J., Cohen, S., 1979. Direct visualization of the binding and internalization of a ferritin conjugate of epidermal growth factor in human carcinoma cells A-431. *Journal of Cell Biology* 81 (2), 382–395.
- [10] Haugh, J.M., 2002. A unified model for signal transduction reactions in cellular membranes. *Biophysical Journal* 82, 591–604.
- [11] Herbst, R.S., 2004. Review of epidermal growth factor receptor biology. *International Journal of Radiation Oncology Biology Physics* 59 (2), 21–26.
- [12] Holbro, T., Hynes, N.E., 2004. ErbB receptors: directing key signaling networks throughout life. *Annual Review of Pharmacology and Toxicology* 44, 195–217.
- [13] Holbrook, M.R., Slakey, L.L., Gross, D.J., 2000. Thermodynamic mixing of molecular states of the epidermal growth factor receptor modulates macroscopic ligand binding affinity. *Biochemical Journal* 352, 99–108.
- [14] Jacobson, K., Sheets, E.D., Simson, R., 1995. Revisiting the fluid mosaic model of membranes. *Science* 268, 1441–1442.
- [15] Jorissen, R.N., Walker, F., Pouliot, N., Garrett, T.P.J., Ward, C.W., Burgess, A.W., 2003. Epidermal growth factor receptor: mechanisms of activation and signalling. *Experimental Cell Research* 284 (1), 31–53.
- [16] Kholodenko, B.N., 2006. Cell-signalling dynamics in time and space. *Nature Reviews Molecular Cell Biology* 7 (3), 165–176.
- [17] Klein, P., Mattoon, D., Lemmon, M.A., Schlessinger, J., 2004. A structurebased model for ligand binding and dimerization of EGF receptors. *Proceedings of the National Academy of Sciences of the USA* 101 (4), 929–934.
- [18] Kusumi, A., Sako, Y., 1996. Cell surface organization by the membrane skeleton. *Current Opinion in Cell Biology* 8 (4), 566–574.
- [19] Kusumi, A., Sako, Y., Yamamoto, M., 1993. Confined lateral diffusion of membrane receptors as studied by single particle tracking (nanovid microscopy). Effects of calcium-induced differentiation in cultured epithelial cells. *Biophysical Journal* 65 (5), 2021–2040.
- [20] Kusumi, A., Nakada, C., Ritchie, K., Murase, K., Suzuki, K., Murakoshi, H., Kasai, R.S., Kondo, J., Fujiwara, T., 2005. Paradigm shift of the plasma membrane concept from the two-dimensional continuum fluid to the partitioned fluid: high-speed single-molecule tracking of membrane molecules. *Annual Review of Biophysics and Biomolecular Structure* 34 (1), 351–378.
- [21] Laude, A.J., Prior, I.A., 2004. Plasma membrane microdomains: organization, function and trafficking (review). *Molecular Membrane Biology* 21, 193–205.
- [22] Lauffenburger, D. A., Linderman, J. J., 1993. *Receptors Models for Binding, Trafficking, and Signaling*. Oxford University Press, New York.
- [23] Lemmon, M. A., Bu, Z., Ladbury, J. E., Zhou, M., Pinchasi, D., Lax, I., Engelman, D. M., Schlessinger, J., 1997. Two EGF molecules contribute additively to stabilization of the EGF dimer. *The EMBO Journal* 16, 281–294.
- [24] Lidke, D.S., Nagy, P., Heintzmann, R., Arndt-Jovin, D.J., Post, J.N., Grecco, H.E., Jares-Erijman, E.A., Jovin, T.M., 2004. Quantum dot ligands provide new insights into erbB/HER receptor-mediated signal transduction. *Nature Biotechnology* 22, 198–203.
- [25] Lommerse, P.H.M., Spaink, H.P., Schmidt, T., 2004. In vivo plasma membrane organization: results of biophysical approaches. *Biochimica et Biophysica Acta (BBA)—Biomembranes* 1664 (2), 119–131.
- [26] Ma'ayan, A., Blitzer, R.D., Iyengar, R., 2005. Toward predictive models of mammalian cells. *Annual Review of Biophysics and Biomolecular Structure* 34 (1), 319–349.
- [27] Martin-Fernandez, M., Clarke, D. T., Tobin, M. J., Jones, S. V., Jones, G. R., 2002. Preformed oligomeric epidermal growth factor receptors undergo an ectodomain structure change during signaling. *Biophysical Journal* 82 (5), 2415–2427.
- [28] Maxfield, F. R., 2002. Plasma membrane microdomains. *Current Opinion in Cell Biology* 14 (4), 483–487.
- [29] Mayawala, K., Vlachos, D. G., Edwards, J. S., 2005a. Heterogeneities in EGF receptor density at the cell surface can lead to concave up Scatchard plot of EGF binding. *FEBS Letters* 579 (14), 3043–3047.
- [30] Mayawala, K., Vlachos, D. G., Edwards, J. S., 2005b. Computational modeling reveals molecular details of epidermal growth factor binding. *BMC Cell Biology* 6, 41.
- [31] Mayawala, K., Vlachos, D. G., Edwards, J. S., 2006. Spatial modeling of dimerization reaction dynamics in the plasma membrane: Monte Carlo vs. continuum differential equations. *Biophysical Chemistry* 121 (3), 194–208.
- [32] Miller, K., Beardmore, J., Kanety, H., Schlessinger, J., Hopkins, C., 1986. Localization of the epidermal growth factor (EGF) receptor within the endosome of EGF-stimulated epidermoid carcinoma (A431) cells. *Journal of Cell Biology* 102 (2), 500–509.
- [33] Monine, M. I., Haugh, J. M., 2005. Reactions on cell membranes: comparison of continuum theory and Brownian dynamics simulations. *The Journal of Chemical Physics* 123, 074908.
- [34] Monine, M. I., Berezhkovskii, A. M., Joslin, E. J., Wiley, H. S., Lauffenburger, D. A., Shvartsman, S. Y., 2005. Ligand accumulation in autocrine cell cultures. *Biophysical Journal* 88 (4), 2384–2390.
- [35] Moriki, T., Maruyama, H., Maruyama, I. N., 2001. Activation of preformed EGf receptor dimers by ligand-induced rotation of the transmembrane domain1. *Journal of Molecular Biology* 311 (5), 1011–1026.
- [36] Murakoshi, H., Iino, R., Kobayashi, T., Fujiwara, T., Ohshima, C., Yoshimura, A., Kusumi, A., 2004. Single-molecule imaging analysis of Ras activation in living cells. *Proceedings of the National Academy Sciences of the USA* 101 (19), 7317–7322.
- [37] Murase, K., Fujiwara, T., Umemura, Y., Suzuki, K., Iino, R., Yamashita, H., Saito, M., Murakoshi, H., Ritchie, K., Kusumi, A., 2004. Ultrafine membrane compartments for molecular diffusion as revealed by single molecule techniques. *Biophysical Journal* 86 (6), 4075–4093.
- [38] Normanno, N., De Luca, A., Bianco, C., Strizzi, L., Mancino, M., Maiello, M. R., Carotenuto, A., De Feo, G., Caponigro, F., Salomon, D.S., 2006. Epidermal growth factor receptor (EGFR) signaling in cancer. *Gene* 366(1), 2–16.
- [39] Parton, R.G., Hancock, J.F., 2004. Lipid rafts and plasma membrane microorganization: insights from Ras. *Trends in Cell Biology* 14 (3), 141–147.
- [40] Pike, L.J., 2003. Lipid rafts: bringing order to chaos. *Journal of Lipid Research* 44 (4), 655–667.
- [41] Pribyl, M., Muratov, C.B., Shvartsman, S.Y., 2003. Long-range signal transmission in autocrine relays. *Bio-*

- physical Journal 84 (2), 883–896.
- [42] Rees, A. R., Gregoriou, M., Johnson, P., Garland, P. B., 1984. High affinity epidermal growth factor receptors on the surface of A431 cells have restricted lateral diffusion. *The EMBO Journal* 3, 1843–1847.
- [43] Reese, J. S., Raimondeau, S., Vlachos, D.G., 2001. Monte Carlo algorithms for complex surface reaction mechanisms: efficiency and accuracy. *Journal of Computational Physics* 173, 302–321.
- [44] Roy, C. L., Wrana, J. L., 2005. Clathrin- and non-clathrin-mediated endocytic regulation of cell signaling. *Nature Reviews Molecular Cell Biology* 6, 112–126.
- [45] Sako, Y., Minoghchi, S., Yanagida, T., 2000. Single-molecule imaging of EGFR signalling on the surface of living cells. *Nature Cell Biology* 2 (3), 168–172.
- [46] Scatchard, G., 1949. The attractions of proteins for small molecules and ions. *Annals of the New York Academy of Sciences* 51 (4), 660–672.
- [47] Schlessinger, J., 1986. Allosteric regulation of the epidermal growth factor receptor kinase. *Journal of Cell Biology* 103 (6), 2067–2072.
- [48] Sherrill, J. M., Kyte, J., 1996. Activation of epidermal growth factor receptor by epidermal growth factor. *Biochemistry* 35, 5705–5718.
- [49] Shvartsman, S. Y., Wiley, H. S., Lauffenburger, D. A., 2004. Epidermal growth factor receptor signaling in tissues. *IEEE Control Systems Magazine* 24 (4), 53–61.
- [50] Simons, K., Toomre, D., 2000. Lipid rafts and signal transduction. *Nature Reviews Molecular Cell Biology* 1, 31–39.
- [51] Singer, S. J., Nicolson, G. L., 1972. Fluid mosaic model of structure of cell membranes. *Science* 175 (4023), 720–731.
- [52] Torney, D. C., McConnell, H. M., 1983. Diffusion-limited reaction theory for two-dimensional systems. *Proceedings of the Royal Society of London Series A*. 387, 147–170.
- [53] Vanbelzen, N., Rijken, P. J., Hage, W. J., Delaat, S. W., Verkleij, A. J., Boonstra, J., 1988. Direct visualization and quantitative-analysis of epidermal growth factor-induced receptor clustering. *Journal of Cellular Physiology* 134, 413–420.
- [54] Vereb, G., Szollosi, J., Matko, J., Nagy, P., Farkas, T., Vigh, L., Matyus, L., Waldmann, T.A., Damjanovich, S., 2003. Dynamic, yet structured: the cell membrane three decades after the Singer–Nicolson model. *Proceedings of the National Academy of Sciences of the USA* 100 (14), 8053–8058.
- [55] Verveer, P. J., Wouters, F. S., Reynolds, A. R., Bastiaens, P. I. H., 2000. Quantitative imaging of lateral ErbB1 receptor signal propagation in the plasma membrane. *Science* 290 (5496), 1567–1570.
- [56] Vlachos, D.G., 2005. A review of multiscale analysis: examples from systems biology, materials engineering, and other fluid–surface interacting systems. *Advances in Chemical Engineering* 30, 1–61.
- [57] Vlachos, D.G. 2007. Temporal coarse-graining of microscopic lattice kinetic Monte Carlo simulations via -leaping, in preparation.
- [58] Weijer, C.J., 2003. Visualizing signals moving in cells. *Science* 300, 96–100.
- [59] Wiley, H.S., 1988. Anomalous binding of epidermal growth factor to A431 cells is due to the effect of high receptor densities and a saturable endocytic system. *Journal of Cell Biology* 107 (2), 801–810.
- [60] Wiley, H. S., Shvartsman, S. Y., Lauffenburger, D. A., 2003. Computational modeling of the EGF-receptor system: a paradigm for systems biology. *Trends in Cell Biology* 13 (1), 43–50.
- [61] Wilson, B. S., Steinberg, S. L., Liederman, K., Pfeiffer, J. R., Surviladze, Z., Zhang, J., Samelson, L. E., Yang, L.-h., Kotula, P. G., Oliver, J. M., 2004. Markers for detergent-resistant lipid rafts occupy distinct and dynamic domains in native membranes. *Molecular Biology Cell* 15 (6), 2580–2592.
- [62] Wofsy, C., Goldstein, B., 1992. Interpretation of Scatchard plots for aggregating receptor systems. *Mathematical Biosciences* 112 (1), 115–154.
- [63] Wofsy, C., Goldstein, B., Lund, K., Wiley, H., 1992. Implications of epidermal growth factor (EGF) induced EGF receptor aggregation. *Biophysical Journal* 63 (1), 98–110.
- [64] Woolf, P.J., Linderman, J. J., 2003. Untangling ligand induced activation and desensitization of G-protein-coupled receptors. *Biophysical Journal* 84 (1), 3–13.
- [65] Yarden, Y., Sliwkowski, M. X., 2001. Untangling the ErbB signalling network. *Nature Reviews Molecular Cell Biology* 2, 127–137.
- [66] Yu, X., Sharma, K. D., Takahashi, T., Iwamoto, R., Mekada, E., 2002. Ligand-independent dimer formation of epidermal growth factor receptor (EGFR) is a step separable from ligand-induced EGFR signaling. *Molecular Biology of the Cell* 13 (7), 2547–2557.
- [67] Zidovetzki, R., Johnson, D. A., Arndt-Jovin, D. J., Jovin, T. M., 1991. Rotational mobility of high-affinity epidermal growth factor receptors on the surface of living A431 cells. *Biochemistry* 30, 6162–6166.
- [68] Ziff, R. M., Gulari, E., Barshad, Y., 1986. Kinetic phase transitions in an irreversible surface-reaction model. *Physical Review Letters* 56, 2553–2556.